

Reactions of substituted benzylidene Meldrum's acids and methylthiobenzylidene Meldrum's acids with OH^- , $\text{CF}_3\text{CH}_2\text{O}^-$ and $\text{HOCH}_2\text{CH}_2\text{S}^-$ in 50% DMSO–50% water. π -Donor effects, soft acid–base interactions and transition state imbalances

Claude F. Bernasconi,^{*†} Rodney J. Ketner,[†] Xin Chen[‡], and Zvi Rappoport[‡]

[†]*Department of Chemistry and Biochemistry, University of California, Santa Cruz, California 95064*

[‡]*Department of Organic Chemistry, The Hebrew University of Jerusalem, Jerusalem 91904, Israel*

E-mail: bernasconi@chemistry.ucsc.edu

Dedicated to Professor Oswald S. Tee on the occasion of his 60th birthday, and in recognition of his many contributions to chemistry in Canada

(received 28 Aug 01; accepted 24 Jan 02; published on the web 01 Feb 02)

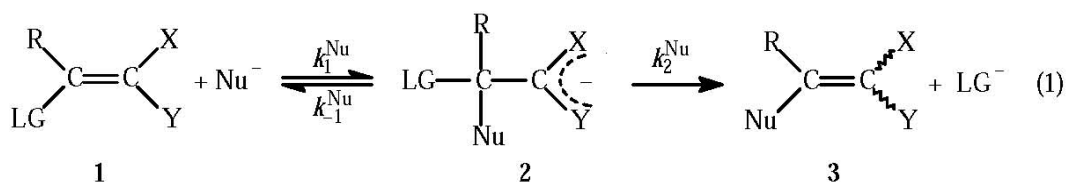
Abstract

A kinetic study of the reactions of phenyl substituted benzylidene Meldrum's acids (**5-H-Z** with Z = 4-MeO, 4-Me, H, 4-Br, 3-Cl and 4-NO₂) and methylthiobenzylidene Meldrum's acids (**5-SMe-Z** with Z = 4-MeO, 4-Me, H, 4-Br, 4-CF₃ and 3,5-(CF₃)₂) with OH^- , $\text{CF}_3\text{CH}_2\text{O}^-$ and $\text{HOCH}_2\text{CH}_2\text{S}^-$ in 50% DMSO–50% water (v/v) at 20 °C is reported. The reactions of **5-H-Z** lead to reversible attachment of the nucleophile to the substrate; with $\text{CF}_3\text{CH}_2\text{O}^-$ and $\text{HOCH}_2\text{CH}_2\text{S}^-$ rate (k_1^{Nu} and k_{-1}^{Nu}) and equilibrium constants (K_1^{Nu}) for this process could be determined while for the reactions with OH^- only k_1^{Nu} was obtained. The reactions of **5-SMe-Z** lead to substitution of the MeS group by the nucleophile via a two-step mechanism. With $\text{HOCH}_2\text{CH}_2\text{S}^-$ the first step represents rapid reversible nucleophilic attachment to the substrate which is followed by slow leaving group departure (k_2^{Nu}). Rate (k_1^{Nu} , k_{-1}^{Nu} , k_2^{Nu}) and equilibrium constants (K_1^{Nu}) could be determined. With $\text{CF}_3\text{CH}_2\text{O}^-$ the kinetic behavior is similar to that with $\text{HOCH}_2\text{CH}_2\text{S}^-$ but complications leave some ambiguity about the interpretation of some of the rate data and hence only k_1^{Nu} is reported. With OH^- the nucleophilic attachment step is rate limiting and hence only k_1^{Nu} could be obtained. Substituent effects on the various rate and equilibrium constants were analyzed by the Hammett and Brønsted equations and provided insights into the π -donor effects of the MeS (leaving group) and the 4-MeO group (substituent) as well as into their mutual interaction, the presence of transition state imbalances, and the effect of soft acid–soft base interactions.

Keywords: Arylidene Meldrum's acid, kinetic study, transition state imbalances, oxygen and sulfur nucleophiles

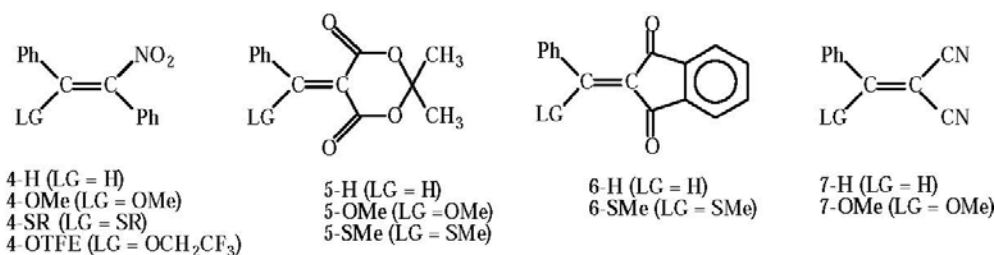
Introduction

In a series of recent papers we have reported kinetic studies of nucleophilic vinylic substitution (S_NV) reactions that proceed by the attachment–detachment mechanism (eq 1) typical for substrates activated by electron withdrawing groups



Nu = nucleophile; LG = leaving group

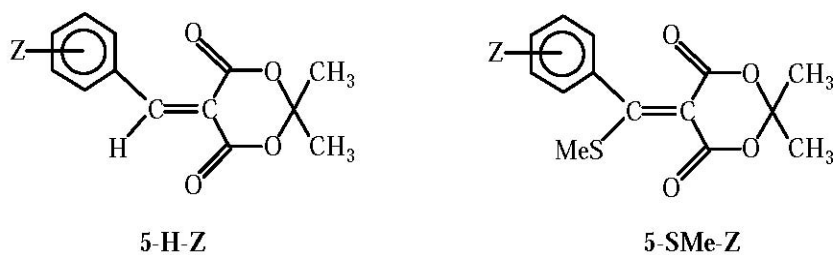
(X, Y).¹⁻¹³ We have focused mainly on reactions where the intermediate (**2**) accumulates to detectable levels^{1,2,5-9,11-13} because this allows the determination of all individual rate constants (k_1^{Nu} , k_{-1}^{Nu} and k_2^{Nu}). Some representative systems studied to date are the reactions of **4-LG**, **5-LG**, **6-LG** and **7-LG** with alkoxide and thiolate ions as well as amines in 50% DMSO–50% water at 20 °C.



A major reason why **2** accumulates to detectable levels in these reactions is that the π -acceptor groups (X, Y) provide the necessary stabilization of the intermediate by delocalizing the negative charge. This implies that the formation of **2** should show some of the characteristic features of reactions that lead to resonance stabilized anions in general. One such feature is the relatively high intrinsic barrier or low intrinsic rate constant,¹⁴ especially for substrates with strong π -acceptors.¹⁵⁻¹⁷ Another is imbalanced transition states in the sense that charge delocalization into X, Y lags behind bond formation between carbon and the nucleophiles.¹⁵⁻¹⁷

What complicates the reactivity patterns is that other factors such as the π -donor ability of

the leaving group, steric effects and anomeric effects¹⁸ play an important role as well. Nevertheless, there is an accumulating database that confirms the expected correlation between intrinsic barriers and π -acceptor strength for these reactions but there is only a relatively small number of investigations that address the question of transition state imbalance. Information about the latter comes from the study of substituent effects that provide Brønsted-type structure-reactivity coefficients such as $\alpha_{nuc}^n = \text{dlog } k_1^{Nu} / \text{dlog } K_1^{Nu}$ (variation of phenyl substituent of the vinylic substrate) and $\beta_{nuc}^n = \text{dlog } k_1^{Nu} / \text{dlog } K_1^{Nu}$ (variation of the pK_a of the nucleophile). This paper presents results of an investigation of substituent effects on the reactions of **5-H-Z** ($Z = 4\text{-MeO}, 4\text{-Me}, \text{H}, 4\text{-Br}, 3\text{-Cl}$ and 4-NO_2) and **5-SMe-Z** ($Z = 4\text{-MeO}, 4\text{-Me}, \text{H}, 4\text{-Br}, 4\text{-CF}_3$ and $3,5\text{-(CF}_3)_2$) with OH^- , $\text{CF}_3\text{CH}_2\text{O}^-$ and $\text{HOCH}_2\text{CH}_2\text{S}^-$ in 50% DMSO–50% water (v/v) at 20 °C.



Apart from addressing the issue of transition state imbalances, our results also allow an assessment under what conditions the π -donor effect of a para methoxy group is effective or ineffective. Furthermore, some of our data suggest the operation of the hard-soft acid-base principle.²⁴

Results

General Procedures. All kinetic experiments were performed in 50% DMSO–50% water (v/v) at 20 °C and conducted under pseudo-first-order conditions with the vinylic substrates as the minor component. The basic features of the kinetic experiments were quite similar to those for the reactions of the parent substrates ($Z = \text{H}$) with OH^- , $\text{CF}_3\text{CH}_2\text{O}^-$ and $\text{HOCH}_2\text{CH}_2\text{S}^-$, respectively, reported earlier^{11,25} and hence only an abbreviated account is given here. For the reactions of **5-H-Z** there is no k_2^{Nu} -step (eq 1) because H is not a real leaving group and hence only data on the nucleophilic attachment step were obtained.

For the reactions of **5-SMe-Z** with $\text{HOCH}_2\text{CH}_2\text{S}^-$ the intermediate accumulates to detectable levels and all rate constants in eq 1 could be determined. For the reactions of **5-SMe-Z** with $\text{CF}_3\text{CH}_2\text{O}^-$ the kinetic results are similar to those for the reactions with $\text{HOCH}_2\text{CH}_2\text{S}^-$ but some ambiguities as to the nature of the second phase of the reaction render an interpretation of the data difficult.¹¹ For the reactions of **5-SMe-Z** with OH^- the breakdown of the intermediate to products is faster than its formation and hence only k_1^{Nu} could be measured.¹¹

All the rate and equilibrium constants determined in this study are summarized in Tables 1 (**5-H-Z**) and 2 (**5-SMe-Z**). In the following sections the individual reactions are briefly described.

Reactions of 5-H-Z with OH⁻. The reaction refers to eq 2 and the observed pseudo-first-order rate constants are given by eq 3. Plots of k_{obsd} vs. $[\text{OH}^-]$ were obtained in the $[\text{OH}^-]$ range from 0.015 to 0.10 M (6 points) from which k_1^{OH} was determined; the intercepts were too small for a determination of k_{-1} .

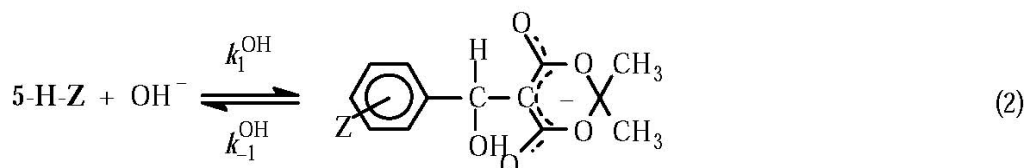


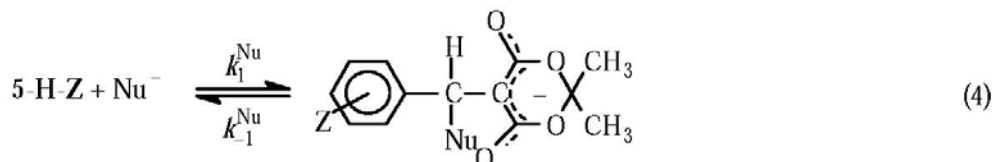
Table 1. Rate and Equilibrium Constants for the Reactions of **5-H-Z** with OH⁻, CF₃CH₂O⁻ and HOCH₂CH₂S⁻ in 50% DMSO–50% water (v/v) at 20 °C, $\mu = 0.5$ M (KCl).

Z	k_1^{Nu} M ⁻¹ s ⁻¹	k_{-1}^{Nu} s ⁻¹	k_1^{Nu} M ⁻¹
Nu = OH ⁻			
4-MeO	$(5.28 \pm 0.06) \times 10^2$		
4-Me	$(9.84 \pm 0.11) \times 10^2$		
H ^a	$(1.80 \pm 0.02) \times 10^3$		
4-Br	$(3.35 \pm 0.11) \times 10^3$		
3-Cl	$(4.83 \pm 0.11) \times 10^3$		
4-NO ₂	$(1.23 \pm 0.08) \times 10^4$		
Nu = CF ₃ CH ₂ O ⁻ (TfO ⁻)			
4-MeO	$(6.74 \pm 0.16) \times 10^3$	$(1.77 \pm 0.21) \times 10^{-2}$	$(3.81 \pm 0.53) \times 10^5$
4-Me	$(1.20 \pm 0.04) \times 10^4$	$(6.21 \pm 0.03) \times 10^{-3}$	$(1.93 \pm 0.07) \times 10^6$
H ^a	$(2.06 \pm 0.08) \times 10^4$	$(3.25 \pm 0.54) \times 10^{-3}$	$(6.34 \pm 1.26) \times 10^6$
4-Br	$(3.98 \pm 0.07) \times 10^4$	$(1.83 \pm 0.10) \times 10^{-3}$	$(2.17 \pm 0.16) \times 10^7$
3-Cl	$(4.44 \pm 0.20) \times 10^4$	$(1.09 \pm 0.26) \times 10^{-3}$	$(4.07 \pm 1.13) \times 10^7$
4-NO ₂	$(1.08 \pm 0.01) \times 10^5$	$(4.47 \pm 0.14) \times 10^{-4}$	$(2.42 \pm 0.10) \times 10^8$
Nu = HOCH ₂ CH ₂ S ⁻ (RS ⁻)			
	$(5.85 \pm 0.09) \times 10^6$	$(1.73 \pm 0.15) \times 10^{-3}$	$(3.39 \pm 0.24) \times 10^9$
	$(8.60 \pm 0.11) \times 10^6$	$(5.55 \pm 1.38) \times 10^{-4}$	$(1.55 \pm 0.38) \times 10^{10}$
	$(1.44 \pm 0.13) \times 10^7$	$(2.68 \pm 0.32) \times 10^{-4}$	$(5.38 \pm 0.17) \times 10^{10}$
	$(2.37 \pm 0.01) \times 10^7$	$(1.30 \pm 0.10) \times 10^{-4}$	$(1.82 \pm 0.13) \times 10^{11}$
	$(2.84 \pm 0.04) \times 10^7$	$(8.38 \pm 1.34) \times 10^{-5}$	$(3.39 \pm 0.50) \times 10^{11}$
	$(7.82 \pm 0.14) \times 10^7$	$(8.77 \pm 1.88) \times 10^{-6}$	$(8.91 \pm 1.78) \times 10^{12}$

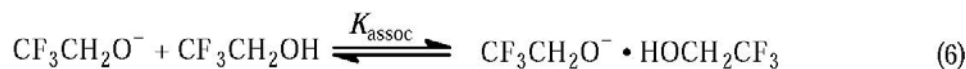
^a Reference 25.

$$k_{\text{obsd}} = k_1^{\text{OH}}[\text{OH}^-] + k_{-1}^{\text{OH}} \quad (3)$$

Reactions of 5-H-Z with $\text{CF}_3\text{CH}_2\text{O}^-$ and $\text{HOCH}_2\text{CH}_2\text{S}^-$. The reactions are shown in eq 4 with $\text{Nu}^- = \text{CF}_3\text{CH}_2\text{O}^-$ or $\text{HOCH}_2\text{CH}_2\text{S}^-$; k_{obsd} is given by eq 5. With $\text{CF}_3\text{CH}_2\text{O}^-$, the reactions were run in trifluoroethanol buffers at pH values between 13.15 and 13.39. In calculating the free $\text{CF}_3\text{CH}_2\text{O}^-$ (TFEO) concentration, the homo-association equilibrium (eq 6, $K_{\text{assoc}} = 1.8 \text{ M}^{-1}$)⁶ was taken into account. Plots of k_{obsd}



$$k_{\text{obsd}} = k_1^{\text{Nu}}[\text{Nu}^-] + k_{-1}^{\text{Nu}} \quad (5)$$

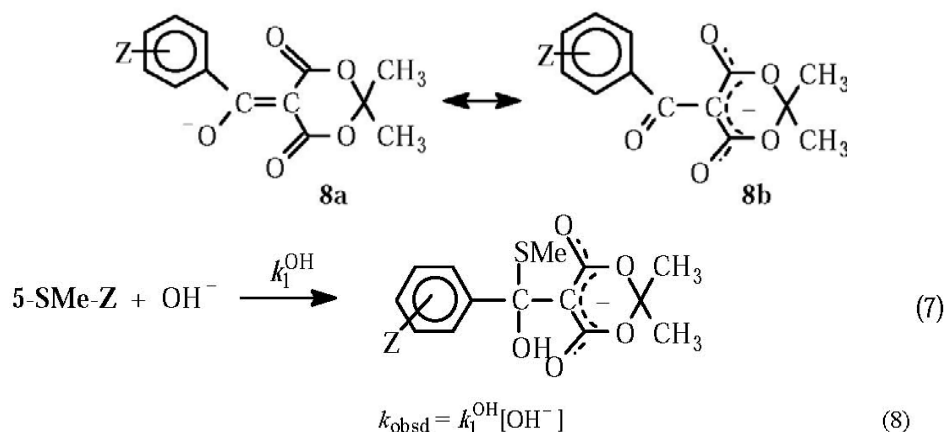


vs. $[\text{CF}_3\text{CH}_2\text{O}^-]$ with concentrations ranging from about 2.5×10^{-3} to about 2.2×10^{-3} M (6 points) were linear and yielded k_1^{TFEO} ; the intercepts were too small for an accurate determination of k_{-1}^{TFEO} . However, k_{-1}^{TFEO} could be determined by following the breakdown of the intermediate—generated at high pH—in a triethylamine buffer at 10.5. At this pH eq 4 favors the reactants and eq 5 simplifies to $k_{\text{obsd}} \approx k_{-1}^{\text{TFEO}}$

We also examined the possibility of general acid catalysis of $\text{CF}_3\text{CH}_2\text{O}^-$ expulsion by Et_3NH^+ by running the reaction at several $[\text{Et}_3\text{NH}^+]$ from 0.006 to 0.03 M. Within this range k_{obsd} increased slightly with increasing $[\text{Et}_3\text{NH}^+]$ for some substrates and decreased slightly for some other substrates, but no consistent pattern emerged and hence the reported k_{-1}^{TFEO} values represent averages of k_{obsd} .

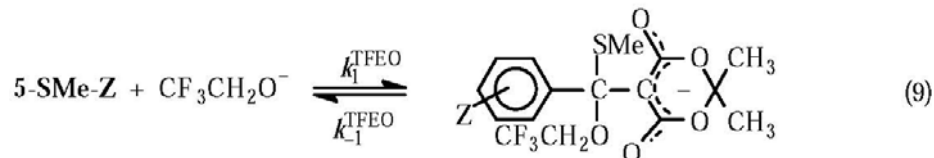
Due to the high reactivity of $\text{HOCH}_2\text{CH}_2\text{S}^-$, its reactions with **5-H-Z** had to be run at pH 7.34, a pH well below the $\text{p}K_a$ (10.57) of $\text{HOCH}_2\text{CH}_2\text{SH}$, in order to keep the free $\text{HOCH}_2\text{CH}_2\text{S}^-$ concentrations low. This pH was maintained with an N-methylmorpholine buffer. Even at this pH, the intercepts of the plots according to eq 5 were too small to yield reliable k_{-1}^{RS} values in the $[\text{HOCH}_2\text{CH}_2\text{S}^-]$ range from 1.1×10^{-6} to 1.6×10^{-5} M (8 points). In this case, k_{-1}^{RS} was obtained as $k_{-1}^{\text{RS}} = k_1^{\text{RS}} / K_1^{\text{RS}}$ with K_1^{RS} being the equilibrium constant; the K_1^{RS} values were obtained in chloroacetate buffers or HCl solution by applying classical spectrophotometric methodology.

Reactions of 5-SMe-Z with OH⁻. As shown previously for **5-SMe**,¹¹ the reaction with OH⁻ leads to the corresponding substitution product which, under most conditions, is ionized and is best represented as the enolate **8a** ↔ **8b**.⁹ The rate limiting step is nucleophilic attachment of OH⁻ to **5-SMe**, eq 7 and hence k_{obsd} is given by eq 8. Data were obtained in [OH⁻] range from 0.04 to 0.24 M (6 points).



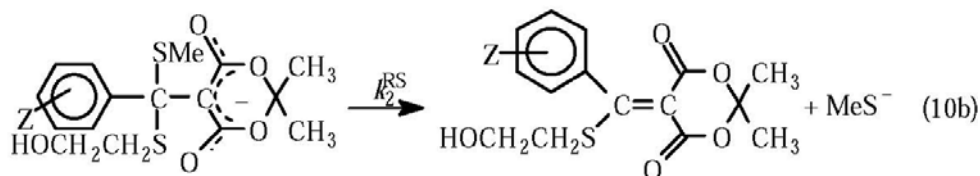
Reactions of 5-SMe-Z with CF₃CH₂O⁻. As described earlier,¹¹ the reaction of **5-SMe** with CF₃CH₂O⁻ buffers is characterized by two kinetic processes²⁶; the same is true for the substituted derivatives. This process could be observed at 335 nm (loss of **5-SMe**) as well as at 260 nm (formation of the intermediate). The data at 335 nm were of better quality and hence the results obtained at this wavelength were used in our kinetic analysis. Plots of k_{obsd} vs. [CF₃CH₂O⁻] obtained at pH 14.6 (ca. 1.3×10^{-2} to 1.9×10^{-1} M, 8 points) were linear either without intercept or with a small one. The slopes correspond to k_1^{TFCO} . The interpretation of the intercepts is ambiguous because they represent a complex combination of contributions from k_{-1}^{TFCO} and a k_1^{OH} [OH⁻] term from the reaction with OH⁻.²⁶ Hence no kinetic information was extracted from these intercepts.

The second process was only observed at 260 nm (loss of the intermediate); it is much slower than the first. As discussed earlier,¹¹ it is not clear what reaction this process is referring to; even though the dependence of k_{obsd} on [CF₃CH₂O⁻] is consistent with rapid equilibrium formation of the intermediate shown in eq 9 followed by rate limiting



conversion of the intermediate to products,²⁸ the spectral changes associated with this process imply a more complex and poorly understood reaction. We therefore refrain from analyzing the kinetic data.

Reactions of 5-SMe-Z with HOCH₂CH₂S⁻. The kinetic behavior of these reactions is similar to that for the reactions of 5-SMe-Z with CF₃CH₂O⁻, i.e. there is a fast process leading to the formation of the corresponding intermediate (eq 10) followed by a slow process, where now intermediate formation represents a fast preequilibrium and product formation is rate limiting (eqs 10a and 10b); in this case the spectral evidence is fully consistent with this interpretation.¹¹



The fast process was studied at pH 10.55 and 10.60. Plots of k_{obsd} vs. [HOCH₂CH₂S⁻], in a [HOCH₂CH₂S⁻] range from 10⁻³ to 1.3 × 10⁻¹ M (10–12 points), yielded straight lines according to eq 11; for Z = MeO and Me the intercepts were large

$$k_{\text{obsd}} = k_1^{\text{RS}} [\text{HOCH}_2\text{CH}_2\text{S}^-] + k_{-1}^{\text{RS}} \quad (11)$$

enough to yield a k_{-1}^{RS} value. For Z = 4-Br, 4-CF₃ and 3,5-(CF₃)₂ measurable intercepts were obtained at pH 9.0 where lower [HOCH₂CH₂S⁻] (7.6 × 10⁻⁶ to 1.5 × 10⁻⁵ M) could be used by buffering the solutions with DABCO.

The slow process was studied at pH 10.55 and 10.60 for Z = 4-MeO, 4-Me, 4-Br and at pH 9.0 for Z = 4-Br, 4-CF₃ and 3,5-(CF₃)₂. It conforms to eq 12; Fig. 1 shows a representative plot of k_{obsd} vs. [HOCH₂CH₂S]. Least squares analysis of the data allowed a determination of k_1^{RS} and k_2^{RS} . In those cases where k_1^{RS} could be determined from eq 12 the agreement with k_1^{RS} obtained as $k_1^{\text{RS}} / k_{-1}^{\text{RS}}$ is excellent (Table 2).

$$k_{\text{obsd}} = \frac{K_1^{\text{RS}} k_2^{\text{RS}} [\text{HOCH}_2\text{CH}_2\text{S}^-]}{1 + K_1^{\text{RS}} [\text{HOCH}_2\text{CH}_2\text{S}^-]} \quad (12)$$

Discussion

Hammett and Brønsted correlations. Hammett plots are shown in Fig. 2 for the reactions of 5-H-Z and 5-SMe-Z with OH⁻ (k_1^{OH}) and of 5-SMe-Z with CF₃CH₂O⁻ (k_1^{TFCO}), in Fig. 3 for the

reactions of **5-H-Z** with $\text{CF}_3\text{CH}_2\text{O}(K_1^{\text{TfEO}}, k_1^{\text{TfEO}}, k_{-1}^{\text{TfEO}})$, in Fig. 4 for the reactions of **5-H-Z** with $\text{HOCH}_2\text{CH}_2\text{S}^- (K_1^{\text{RS}}, k_1^{\text{RS}}, k_{-1}^{\text{RS}})$, and in Fig. 5 for the reactions of **5-SMe-Z** with $\text{HOCH}_2\text{CH}_2\text{S}^- (K_1^{\text{RS}}, k_1^{\text{RS}}, k_{-1}^{\text{RS}}, k_2^{\text{RS}})$. The correlations are good except that in most cases the points for $Z = 4\text{-MeO}$ deviate from the least squares line defined by the other substituents, a feature discussed below. The ρ values summarized in Table 3 were obtained by omitting the 4-MeO substituents from the correlations.

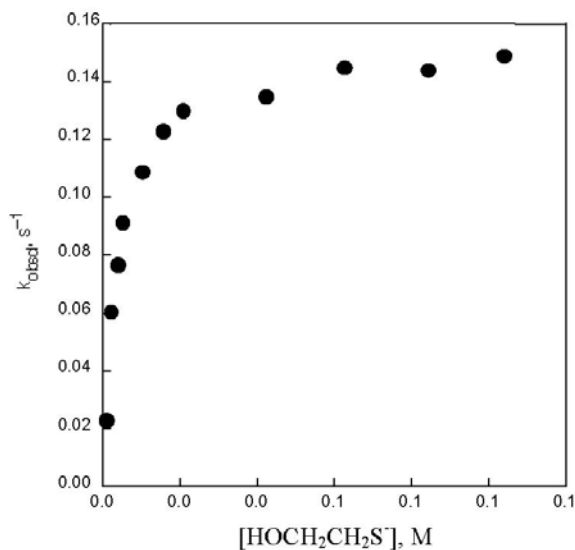


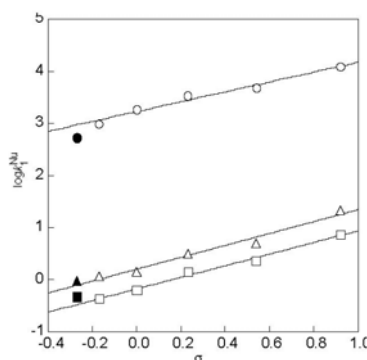
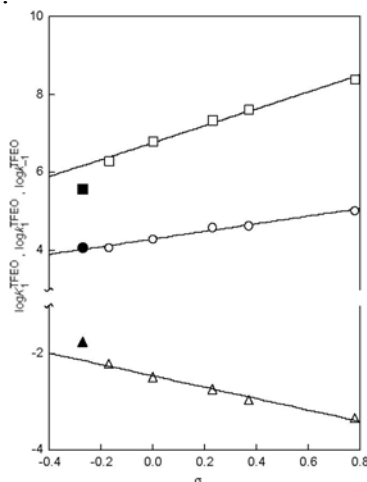
Figure 1. Reaction of **5-SMe-Me** with $\text{HOCH}_2\text{CH}_2\text{S}^-$. Plot of k_{obsd} vs. $[\text{HOCH}_2\text{CH}_2\text{S}^-]$ for the slow process according to eq 12.

Table 2. Rate and Equilibrium Constants for the Reactions of **5-SMe-Z** with OH^- , $\text{CF}_3\text{CH}_2\text{O}^-$ and $\text{HOCH}_2\text{CH}_2\text{S}^-$ in 50% DMSO–50% water (v/v) at 20 °C, $\mu = 0.5 \text{ M}$ (KCl).

Z	k_1^{Nu} $\text{M}^{-1} \text{ s}^{-1}$	k_{-1}^{Nu} s^{-1}	$K_1^{\text{Nu}} = k_1^{\text{Nu}} / k_{-1}^{\text{Nu}}$ M^{-1}	K_1^{Nu} (eq 12) M^{-1}	k_2^{Nu} s^{-1}
Nu = OH ⁻					
4-MeO	0.465 ± 0.013				
4-Me	0.416 ± 0.010				
H ^a	0.634 ± 0.006				
4-Br	1.37 ± 0.06				
4-CF ₃	2.31 ± 0.07				
3,5-(CF ₃) ₂	7.17 ± 0.16				
Nu = CF ₃ CH ₂ O ⁻ (TfO ⁻)					
4-MeO	0.941 ± 0.028				
4-Me	1.15 ± 0.07				
H ^a	1.41 ± 0.12				

Table 2. Continued

4-Br	3.18 ± 0.06				
4-CF ₃	4.89 ± 0.11				
3,5-(CF ₃) ₂	20.9 ± 0.4				
		Nu = HOCH ₂ CH ₂ S ⁻			
4-MeO	$(7.21 \pm 0.05) \times 10^2$	3.33 ± 0.34	$(2.17 \pm 0.23) \times 10^2$	$(2.49 \pm 0.26) \times 10^2$	0.179 ± 0.003
4-Me	$(7.57 \pm 0.04) \times 10^2$	3.15 ± 0.25	$(2.40 \pm 0.20) \times 10^2$	$(2.69 \pm 0.21) \times 10^2$	0.162 ± 0.030
H ^a	$(9.22 \pm 0.12) \times 10^2$	2.78 ± 0.25	$(3.32 \pm 0.34) \times 10^2$	$(3.32 \pm 0.27) \times 10^2$	0.115 ± 0.112
4-Br	$(1.96 \pm 0.06) \times 10^3$	1.27 ± 0.03	$(1.54 \pm 0.08) \times 10^3$		0.098 ± 0.004
4-CF ₃	$(3.65 \pm 0.05) \times 10^3$	0.649 ± 0.027	$(5.62 \pm 0.30) \times 10^3$		0.037 ± 0.006
3,5-(CF ₃) ₂	$(1.45 \pm 0.04) \times 10^4$	0.244 ± 0.039	$(5.94 \pm 1.10) \times 10^4$		0.0165 ± 0.003

^a Reference 11.**Figure 2.** Hammett plots for the reactions of **5-H-Z** with OH⁻ ($\log k_1^{OH}$, O), the reactions of **5-SMe-Z** with CF₃CH₂O⁻ ($\log k_1^{TFEO}$, Δ) and the reactions of **5-SMe-Z** with OH⁻ ($\log k_1^{OH}$, □). The filled symbols refer to Z = 4-MeO.**Figure 3.** Hammett plots for the reactions of **5-H-Z** with CF₃CH₂O⁻: $\log k_1^{TFEO}$ (□); $\log k_1^{TFEO}$ (O); $\log k_1^{TFEO}$ (Δ). The filled symbols refer to Z = 4-MeO.

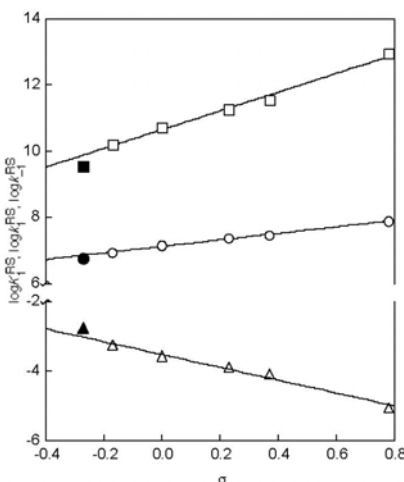


Figure 4. Hammett plots for the reactions of **5-H-Z** with $\text{HOCH}_2\text{CH}_2\text{S}^-$: $\log K_1^{RS}$ (\square); $\log k_1^{RS}$ (\circ); $\log k_{-1}^{RS}$ (Δ). The filled symbols refer to $Z = 4\text{-MeO}$.

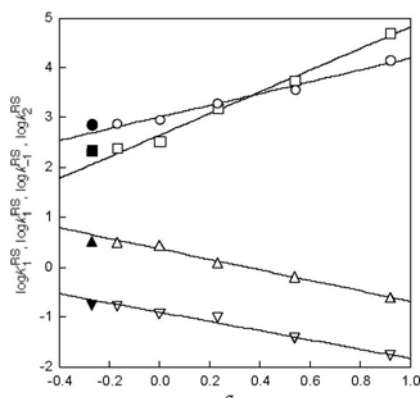


Figure 5. Hammett plots for the reactions of **5-SMe-Z** with $\text{HOCH}_2\text{CH}_2\text{S}^-$: $\log K_1^{RS}$ (\square); $\log k_1^{RS}$ (\circ); $\log k_{-1}^{RS}$ (Δ); $\log k_2^{RS}$ (\square). The filled symbols refer to $Z = 4\text{-MeO}$.

Table 3. Hammett ρ Values^a for the Rate and Equilibrium Constants of the Various Steps of the Reactions of **5-H-Z** and **5-SMe-Z** with OH^- , $\text{CF}_3\text{CH}_2\text{O}^-$ and $\text{HOCH}_2\text{CH}_2\text{S}^-$ in 50% DMSO–50% water (v/v) at 20 °C.

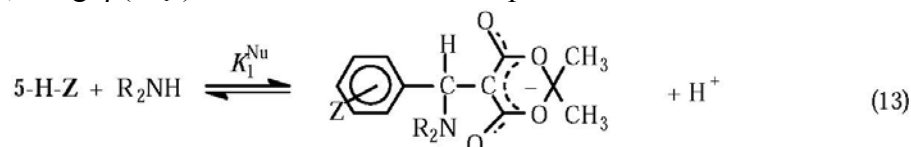
	5-H-Z		
	OH^-	$\text{CF}_3\text{CH}_2\text{O}^-$	$\text{HOCH}_2\text{CH}_2\text{S}^-$
$\rho(K_1^{Nu})$		2.17 ± 0.13 (\downarrow)	2.92 ± 0.20 (\downarrow)
$\rho(k_1^{Nu})$	1.14 ± 0.05 (\downarrow)	0.98 ± 0.08 (\downarrow)	0.98 ± 0.05 (\downarrow)
$\rho(k_{-1}^{Nu})$		-1.19 ± 0.07 (\uparrow)	-1.95 ± 0.18 (\uparrow)
$\rho_n(k_1^{Nu}) = \alpha_{nuc}^n$		0.45 ± 0.02	0.33 ± 0.02

Table 3. Continued

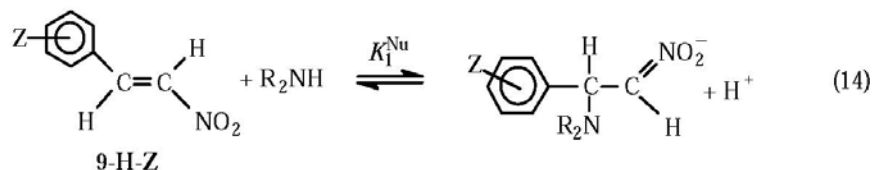
$\rho_n(k_{-1}^{Nu}) = -\alpha_{lg}^n$		-0.55 ± 0.02	-0.67 ± 0.02
$\rho(k_2^{Nu})$			
	5-SMe-Z		
$\rho(K_1^{Nu})$			$2.21 \pm 0.16 (\uparrow)$
$\rho(k_1^{Nu})$	$1.11 \pm 0.06 (\uparrow)$	$1.14 \pm 0.11 (\uparrow)$	$1.18 \pm 0.09 (\uparrow)$
$\rho(k_{-1}^{Nu})$			$-1.05 \pm 0.06 (\downarrow)$
$\rho_n(k_1^{Nu}) = \alpha_{nuc}^n$			0.53 ± 0.01
$\rho_n(k_{-1}^{Nu}) = -\alpha_{lg}^n$			-0.48 ± 0.02
$\rho(k_2^{Nu})$			$-0.90 \pm 0.09 (\downarrow)$

^a The (↓) and (↑) indicate that the point for Z = 4-MeO deviates positively and negatively, respectively, from the Hammett plot.

The $\rho(K_1^{Nu})$ values are all larger than 2, indicating a fairly strong substituent dependence. These values are quite similar to the ones for the reactions of **5-H-Z** with amines to form the anionic adduct, eq 13,²⁹ e.g. $\rho(K_1^{Nu}) = 2.26$ for $R_2NH =$ morpholine.³⁰



The large values imply that the negative charge of the intermediate is relatively close to the substituent and not highly delocalized into the two ester groups, in agreement with independent evidence that charge delocalization plays only a secondary role in the strong stabilization of the Meldrum's acid anion.³¹⁻³⁴ By way of contrast, for morpholine addition to substituted β -nitrostyrenes, eq 14,²⁹ $\rho(K_1^{Nu})$ is much smaller (≈ 1.09),³⁵ consistent with the strong delocalization of the negative charge into the nitro group.



The fact that $\rho(K_1^{Nu})$ for $\text{HOCH}_2\text{CH}_2\text{S}^-$ attachment to **5-SMe-Z** (2.21) is significantly smaller

than for addition of the same nucleophile to **5-H-Z** (2.92) calls for comment. A possible interpretation of this result is that the soft–soft²⁴ acid–base interactions between the thiolate ion and the MeS group in **5-SMe-Z** provide some extra stabilization to the intermediate, thus attenuating the substituent effect on the stability of the intermediate. This is reminiscent of findings in the reaction of thiolate ions with Fischer carbene complexes which were interpreted in a similar way.³⁶

The $\rho(k_1^{Nu})$ values for nucleophilic attack are very similar (0.98 to 1.18) for all reactions, i.e. essentially independent of nucleophile and substrate. The $\rho(k_{-1}^{Nu})$ values for the reverse reaction are similar for the reactions of **5-H-Z** with $\text{CF}_3\text{CH}_2\text{O}^-$ and of **5-SMe-Z** with $\text{HOCH}_2\text{CH}_2\text{S}^-$ (–1.19 and –1.05) but for the reaction of **5-H-Z** with $\text{HOCH}_2\text{CH}_2\text{S}^-$, $\rho(k_{-1}^{Nu}) = -1.95$ is substantially more negative, as required by the higher $\rho(K_1^{Nu})$. The $\rho(k_2^{Nu})$ value for the reaction of **5-SMe-Z** with $\text{HOCH}_2\text{CH}_2\text{S}^-$ (–0.90) is about the same as $\rho(k_{-1}^{Nu})$ (–1.05). This is reasonable since both k_2^{Nu} and k_{-1}^{Nu} refer to the expulsion of a thiolate ion from the intermediate.

Information about the transition state of the first step can be obtained from the *normalized* ρ values, i.e. $\rho_n(k_1^{Nu}) = \rho(k_1^{Nu})/\rho(K_1^{Nu})$ and $\rho_n(k_{-1}^{Nu}) = \rho(k_{-1}^{Nu})/\rho(K_1^{Nu})$; they can also be obtained directly from Brønsted–type plots of $\log k_1^{Nu}$ vs. $\log K_1^{Nu}$ and $\log k_{-1}^{Nu}$ vs. $\log K_1^{Nu}$ (see Fig. 6 for a representative example), with $d\log k_1^{Nu}/d\log K_1^{Nu} = \alpha_{nuc}^n = \rho_n(k_1^{Nu})$ and $d\log k_{-1}^{Nu}/d\log K_1^{Nu} = -\alpha_{lg}^n = \rho_n(k_{-1}^{Nu})$. The α_{nuc}^n values increase from 0.33 for the reactions of **5-H-Z** with $\text{HOCH}_2\text{CH}_2\text{S}^-$ to 0.45 for the reactions of the same substrate with $\text{CF}_3\text{CH}_2\text{O}^-$ to 0.53 for the reactions of **5-SMe-Z** with $\text{HOCH}_2\text{CH}_2\text{S}^-$, suggesting a trend from a somewhat reactant–like to a more central transition state. This trend parallels the decrease in reactivity from high for the reactions of **5-H-Z** with $\text{HOCH}_2\text{CH}_2\text{S}^-$ (for $Z = \text{H}$: $K_1^{Nu} = 5.38 \times 10^{10} \text{ M}^{-1}$, $k_1^{Nu} = 1.44 \times 10^7 \text{ M}^{-1} \text{ s}^{-1}$) to intermediate for the reactions of **5-H-Z** with $\text{CF}_3\text{CH}_2\text{O}^-$ (for $Z = \text{H}$: $K_1^{Nu} = 6.34 \times 10^6 \text{ M}^{-1}$, $k_1^{Nu} = 2.06 \times 10^4 \text{ M}^{-1} \text{ s}^{-1}$) to low for the reaction of **5-SMe-Z** with $\text{HOCH}_2\text{CH}_2\text{S}^-$ (for $Z = \text{H}$: $K_1^{Nu} = 3.32 \times 10^2 \text{ M}^{-1}$, $k_1^{Nu} = 9.22 \times 10^{12} \text{ M}^{-1} \text{ s}^{-1}$); it is consistent with the Hammond–Leffler postulate.^{37,38} A similar trend has been observed for β_{nuc} for the reactions of secondary alicyclic amines with a series of electrophilic alkenes.¹⁶

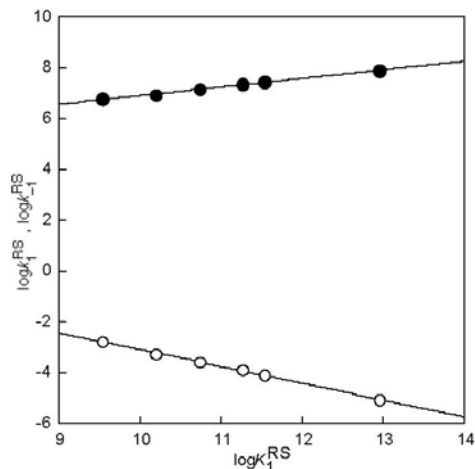
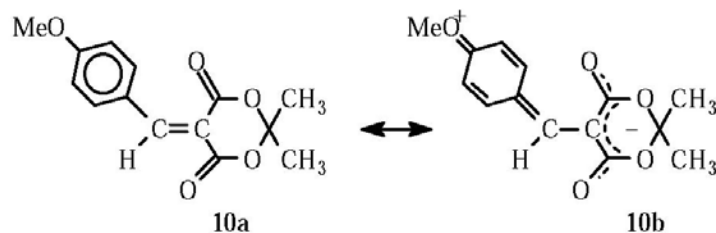


Figure 6. Brønsted-type plots for the reaction of **5-H-Z** with $\text{HOCH}_2\text{CH}_2\text{S}^-$: $\log k_1^{\text{RS}}$ (\bullet); $\log k_{-1}^{\text{RS}}$ (\circ).

Deviations of the 4-MeO substituent. For the reactions of **5-H-Z** the $\log k_1^{\text{Nu}}$ and $\log K_1^{\text{Nu}}$ values for the 4-MeO derivative deviate negatively from the Hammett plots, while the $\log k_{-1}^{\text{Nu}}$ values show a positive deviation (Figs. 2–4). In contrast, for the reactions of **5-SMe-Z**, it is the $\log k_1^{\text{Nu}}$ and $\log K_1^{\text{Nu}}$ values that deviate positively, while $\log k_{-1}^{\text{Nu}}$ falls below the line (Figure 5).

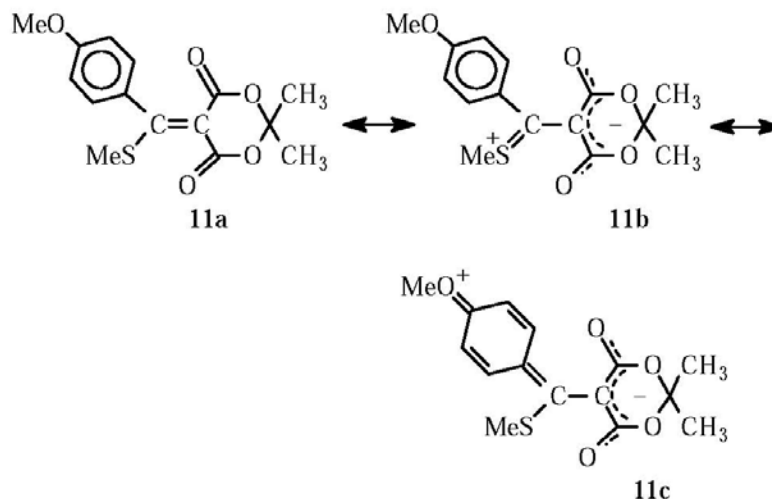
The pattern seen for the reactions of **5-H-Z** with OH^- , $\text{CF}_3\text{CH}_2\text{O}^-$ and $\text{HOCH}_2\text{CH}_2\text{S}^-$ is similar to that observed for the addition of amine nucleophiles to **5-H-Z** as well as to other electrophilic alkenes such as $\text{PhCH}=\text{C}(\text{CN})_2$ ³⁹ and $\text{PhCH}=\text{C}(\text{CH}=\text{O})_2$ ⁴⁰. It can be attributed to the π -donor effect of the 4-MeO group (**10a** \leftrightarrow **10b**) which reduces the reactivity of **5-H-MeO**. This π -donor effect also manifests



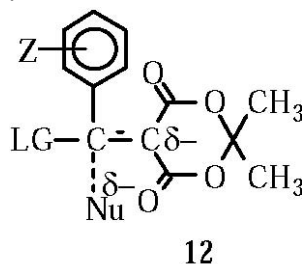
itself in the UV spectrum of **5-H-MeO** whose λ_{max} of 370 nm is much higher than that of the other **5-H-Z** derivatives (4-Me: 334 nm, H: 325 nm, 4-Br: 335 nm, 3-Cl: 316 nm; 4- NO_2 : 318 nm).

With **5-SMe-MeO**, the π -donor effect of the 4-MeO group is reduced; in fact, the reduction is so strong that the electron donating ability of the 4-MeO group is less than that suggested by its Hammett σ value and hence $\log k_1^{\text{Nu}}$ and $\log K_1^{\text{Nu}}$ deviate positively, $\log k_{-1}^{\text{Nu}}$ negatively for the Hammett plots (Figure 5). The most plausible explanation for this reduced π -donor effect is that π -donation by the MeS group (**11a** \leftrightarrow **11b**) is more effective and greatly diminishes the

importance of **11c**. The fact that λ_{\max} (334 nm) for **5-SMe-MeO** is the same as for the other **5-SMe-Z** derivatives (4-Me, H, 4-Br: 334 nm; 4-CF₃ and 3,5-(CF₃)₂: 335 nm) is consistent with our explanation.



Transition state imbalances. One of the major motivations for this study was to learn more about potential transition state imbalances in the nucleophilic attachment steps. Such imbalances where charge delocalization into the π -acceptor group(s) in carbanion forming reactions lags behind bond formation (see, e.g. **12**) appears to be the norm¹⁵⁻¹⁷ and would be expected to occur in the reactions reported in this paper.



They would manifest themselves in α_{nuc}^n values that exceed β_{nuc}^n ; this is because, due to the closer proximity of the negative charge to the Z-substituent at the transition state than in the adduct, the stabilization of the transition state by electron withdrawing substituents is disproportionately strong and hence the substituent effect on k_1^{Nu} is exalted.

Table 4 summarizes α_{nuc}^n and β_{nuc}^n values for the reactions reported in the present study along with the same parameters for similar reactions studied previously. In all cases α_{nuc}^n exceeds β_{nuc}^n , with $I = \alpha_{nuc}^n - \beta_{nuc}^n$ ranging from 0.14 to 0.34. There appears to be a

Table 4. α_{nuc}^n and β_{nuc}^n Values for Nucleophilic Attachment to Various Electrophilic Olefins in 50% DMSO–50% Water (v/v) at 20 °C.

Entry	Substrate		Nucleophile	α_{nuc}^n	β_{nuc}^n	$I = \alpha_{nuc}^n - \beta_{nuc}^n$
1	ArCH=MA ^a	(5-H-Z)	RO ⁻	0.45 ^b	0.25 ^c	0.20
2	ArCH=MA ^a		ArO ⁻	0.59 ^d	0.39 ^d	0.20
3	ArCH=MA ^a	(5-H-Z)	RS ⁻	0.33 ^b	0.19 ^c	0.14
4	ArCH=MA ^a	(5-H-Z)	R ₂ NH	0.25 ^e	0.15 ^e	0.10
5	ArC(SMe)=MA ^a	(5-SMe-Z)	RS ⁻	0.53 ^b	0.19 ^f	0.34
6	ArCH=CHNO ₂	(9-H-Z)	R ₂ NH	0.51 ^g	0.25 ^g	0.26
7	ArCH=C(CN) ₂	(7-H-Z)	R ₂ NH	0.56 ^h	0.42 ^h	0.14

^a MA stands for Meldrum's acid residue. ^b This work. ^c Reference 25. ^d Bernasconi, C. F.; Leonarduzzi, G. D. *J. Am. Chem. Soc.* 1982, *104*, 5133. ^e Reference 30. ^f Reference 11. ^g Reference 35, in water. ^h Reference 39.

complex dependence of the imbalance on the π -acceptor groups, the nature of the nucleophile and on whether or not the substrate has a leaving group. Comparison of entries 4, 6 and 7 suggests that for the same LG the imbalance is relatively large for substrates with strong π -acceptors (NO₂) but small when the π -acceptors are weaker (COOR and CN groups). This is the same pattern observed in the deprotonation of carbon acids activated by the same π -acceptors^{15,17} and reflects the fact that the differences between the charge distribution at the transition state and that of the carbanion increases with the increasing strength of the π -acceptor. Comparison of entries 3 and 5 shows a large increase in the imbalances when the hydrogen is replaced by a MeS group. This increase is the result of a larger α_{nuc}^n value. A possible (speculative) explanation is that a destabilization of the *substrate* by electron withdrawing substituents could enhance α_{nuc}^n . Such a destabilization would occur if the electrostatic interaction of Z with the partial positive charge on the sulfur atom (see **11b**) is stronger than its interaction with the partial negative charge because the latter is partially delocalized. With respect to the dependence of the imbalance on the nucleophile, too many factors such as charge, central atom and size come into play to allow any meaningful conclusions to be drawn.

Conclusions

- (1) The $\rho(K_1^{Nu})$ values are relatively large, consistent with the notion that the negative charge on the respective intermediates or adducts is not particularly strongly delocalized.
- (2) The lower $\rho(K_1^{Nu})$ value for HOCH₂CH₂S⁻ attachment to **5-SMe-Z** compared to **5-H-Z** may

be attributed to a stabilizing soft–soft acid–base interaction in the intermediates derived from **5-SMe-Z**.

(3) For the reactions of **5-H-Z** the $\log k_1^{Nu}$ and $\log K_1^{Nu}$ values for the 4-MeO derivative deviate negatively from the Hammett plots while $\log k_{-1}^{Nu}$ deviates positively. This is the result of the π -donor effect of the MeO group (**10b**). In the reactions of **5-SMe-Z** this effect is greatly diminished because of the π -donor effect of the MeS group (**11b**) and the $\log k_1^{Nu}$ and $\log K_1^{Nu}$ values for the 4-MeO derivatives deviate positively, and the $\log k_{-1}^{Nu}$ values negatively, from the Hammett plots.

(4) The α_{nuc} values increase with decreasing reactivity, suggesting a trend from a somewhat reactant-like transition state to a more central one, as predicted by the Hammond–Leffler postulate.

(5) For all the reactions where α_{nuc} could be determined, α_{nuc} exceeds β_{nuc} , indicating the presence of a transition state imbalance. The size of the imbalance depends on several factors most of which are poorly understood except for a definite trend towards larger imbalances with increasing π -acceptor strength of the activating groups.

Experimental Section

Materials. The substrates in the **5-H-Z** series were prepared as described by Schuster et al.⁴¹ The substrates in the **5-SMe-Z** series were available from a previous study.⁴²

All other materials were from the sources described before.²⁵

Methodology. All procedures, including the spectrophotometric equilibrium determinations, were the same as described in references 9 and 25.

Acknowledgements

This research was supported by grants CHE-9734822 and CHE-0098553 from the National Science Foundation (C.F.B.) and a grant from the U.S.–Israel Binational Science Foundation (Z.R.).

References and Notes

1. Bernasconi, C. F.; Killion, R. B., Jr.; Fassberg, J.; Rappoport, Z. *J. Am. Chem. Soc.* **1989**, *111*, 6862.
2. Bernasconi, C. F.; Fassberg, J.; Killion, R. B., Jr.; Rappoport, Z. *J. Am. Chem. Soc.* **1990**, *112*, 3169.
3. Bernasconi, C. F.; Fassberg, J.; Killion, R. B., Jr.; Rappoport, Z. *J. Org. Chem.* **1990**, *55*, 4568.
4. Bernasconi, C. F.; Fassberg, J.; Killion, R. B., Jr.; Rappoport, Z. *J. Am. Chem. Soc.* **1991**, *113*, 4937.
5. Bernasconi, C. F.; Leyes, A. E.; Rappoport, Z.; Eventova, I. *J. Am. Chem. Soc.* **1993**, *115*, 7513.
6. Bernasconi, C. F.; Schuck, D. F.; Ketner, R. J.; Weiss, M.; Rappoport, Z. *J. Am. Chem. Soc.* **1994**, *116*, 11764.
7. Bernasconi, C. F.; Leyes, A.; Eventova, I.; Rappoport, Z. *J. Am. Chem. Soc.* **1995**, *117*, 1703.
8. Bernasconi, C. F.; Schuck, D. F.; Ketner, R. J.; Eventova, I.; Rappoport, Z. *J. Am. Chem. Soc.* **1995**, *117*, 2719.
9. Bernasconi, C. F.; Ketner, R. J.; Chen, X.; Rappoport, Z. *J. Am. Chem. Soc.* **1998**, *120*, 7461.
10. Bernasconi, C. F.; Leyes, A. E.; Rappoport, Z. *J. Org. Chem.* **1999**, *64*, 2897.
11. Bernasconi, C. F.; Ketner, R. J.; Chen, X.; Rappoport, Z. *Can. J. Chem.* **1999**, *77*, 584.
12. Bernasconi, C. F.; Ketner, R. J.; Brown, S. D.; Chen, X.; Rappoport, Z. *J. Org. Chem.* **1999**, *64*, 8829.
13. Bernasconi, C. F.; Ketner, R. J.; Ragains, M. L.; Chen, X.; Rappoport, Z. *J. Am. Chem. Soc.* **2001**, *123*, 2155.
14. For a reaction with a rate constant k_1 (barrier ΔG_1^\ddagger) in the forward and k_{-1} (ΔG_{-1}^\ddagger) in the reverse direction, the intrinsic rate constant, k_0 (intrinsic barrier ΔG_0^\ddagger), is defined as $k_0 = k_1 = k_{-1}$ ($\Delta G_0^\ddagger = \Delta G_1^\ddagger = \Delta G_{-1}^\ddagger$) where the equilibrium constant $K_1 = 1$ ($\Delta G_0 = 0$).
15. Bernasconi, C. F. *Acc. Chem. Res.* **1987**, *20*, 301; 1992, *25*, 9.
16. Bernasconi, C. F. *Tetrahedron* **1989**, *45*, 4017.
17. Bernasconi, C. F. *Adv. Phys. Org. Chem.* **1992**, *27*, 119.
18. In the present context, the anomeric effect^{19,20} refers to the stabilization exerted by geminal oxygen atoms,²¹⁻²³ e.g. in dialkoxy adducts.
19. Kirby, A. G. *The Anomeric Effect and Related Stereoelectronic Effects of Oxygen*; Springer-Verlag: Berlin, 1983.
20. Schleyer, P. v. R.; Jemmis, E. D.; Spitznagel, G. W. *J. Am. Chem. Soc.* **1985**, *107*, 6393.
21. Hine, J.; Klueppel, A. W. *J. Am. Chem. Soc.* **1974**, *96*, 2924.
22. Wiberg, K. B.; Squires, R. R. *J. Chem. Thermodyn.* **1979**, *11*, 773.
23. Harcourt, M. P.; More O'Ferrall, R. A. *Bull. Soc. Chim. Fr.* **1988**, 407.
24. Pearson, R. G.; Songstad, J. *J. Am. Chem. Soc.* **1967**, *89*, 1827.
25. Bernasconi, C. F.; Ketner, R. J. *J. Org. Chem.* **1998**, *63*, 6266.

26. There is a third process on a much longer time scale which corresponds to hydrolysis.¹¹
27. Bernasconi, C. F. *Relaxation Kinetics*, Academic Press: New York, 1976.
28. k_{obsd} conforms to an equation similar to eq 12.¹¹
29. Note that the reactions with amines involve two steps, the first being the formation of a zwitterionic adduct (K_1'), the second being deprotonation of the zwitterionic adduct (K_a^\pm) to form the anionic adduct shown in eqs 13 and 14. Hence K_1^{Nu} is defined as $K_1' K_a^\pm$ in this case.
30. Bernasconi, C. F.; Panda, M. *J. Org. Chem.* **1987**, *52*, 3042.
31. Arnett, E. M.; Harrelson, J. A., Jr. *J. Am. Chem. Soc.* **1987**, *109*, 809.
32. Wang, X.; Houk, K. N. *J. Am. Chem. Soc.* **1988**, *110*, 1870.
33. Wiberg, K. B.; Laidig, K. E. *J. Am. Chem. Soc.* **1988**, *110*, 1872.
34. Byun, K.; Mo, Y.; Gao, J. *J. Am. Chem. Soc.* **2001**, *123*, 3974.
35. Bernasconi, C. F.; Renfrow, R. A.; Tia, P. R. *J. Am. Chem. Soc.* **1986**, *108*, 4541.
36. Bernasconi, C. F.; Ali, M. *Organometallics* **2001**, *20*, 3383.
37. Hammond, G. S. *J. Am. Chem. Soc.* **1955**, *77*, 334.
38. Leffler, J. E.; Grunwald, E. *Rates and Equilibria of Organic Reactions*; Wiley: New York, 1963; p 128.
39. Bernasconi, C. F.; Killion, R. B., Jr. *J. Org. Chem.* **1989**, *54*, 2878.
40. Bernasconi, C. F.; Flores, F. X.; Claus, J. J.; Dvorak, D. *J. Org. Chem.* **1994**, *59*, 4917.
41. Schuster, P.; Polansky, O. E.; Wesley, F. *Monatsh. Chem.* **1964**, *95*, 53.
42. Beit-Yannai, M.; Chen, X.; Rappoport, Z. *J. Chem. Soc., Perkin 2* **2001**, 1534.